2016

Cofactor Binding Determinants in the NADPH-Dependent Nitrile-Oxidoreductase QueF

Spencer William Cohen
Portland State University

Cofactor binding determinants in the NADPH-dependent nitrile-oxidoreductase QueF

By

Spencer William Cohen

An undergraduate honors thesis submitted in partial fulfillment

of the requirements for the degree of

Bachelor of Science

In

University Honors

And

Biochemistry

Thesis Adviser

Dr. Dirk Iwata-Reuyl

Portland State University

2016

Abstract

The NADPH-dependent nitrile-oxidioreductase, QueF is the only known enzyme capable of reducing a nitrile group to an amine. This ability makes it an attractive alternative to conventional industrial nitrile redution. Understating how QueF binds NADPH may lead to the development of an enzyme capable of using the less expensive reductive cofactor NADH. A cofactor docking model indicates that key residues, Q60 and Y21, interact with the ribose phosphate moiety unique to NADPH. Mutants of these residues (Q60A, Q60N, Q60E, Y21A and Y21F) were developed for steady-state kinetic analysis. Modification to either residue resulted in a decrease in binding and catalytic activity when using NADPH as a hydride source. Q60E had the greatest reduction in activity (0.45% of WT). There appears to be both charge and steric factors involved in direct cofactor binding. Neither WT or mutant enzymes were able to utilize NADH as a reductive cofactor to any observable extent.

Background

Transfer ribonucleic acids (tRNAs) are the adaptor molecules that allow for accurate translation of messenger RNA (mRNA) to peptide. tRNA effectively translates genetic information to peptide by matching the correct amino acid to the genetic information carried by the mRNA in the ribosome[1]. The typical tRNA molecule is L-shaped with an acceptor stem (yellow, Figure 1 left) and an anticodon loop (black, Figure 1 left) on either end. Translation fidelity relies on two important steps. The first is the charging of the particular tRNA with the correct amino acid, accomplished by aminoacyl tRNA synthetases (aaRS)[2]. The second is the matching of the anticodon, the section of RNA that complements the mRNA codon, to the mRNA during translation. There are 20 amino acids that are encoded in the mRNA by 61 distinct triplet codons along with three codons that encode the end of a translation template, known as a STOP codon[3]. This discrepancy between the number of codons and anticodons is referred to as the degeneracy of the genetic code and is allowed largely by chemical modification to nucleotides at positions 34 and 37 of the tRNA (Figure1 right). Position 34 is known as the wobble position, coined by Francis Crick in 1966. Certain nucleotides in the wobble position have the ability to pair with multiple non-cognate bases. Modifications to the nucleotides in the wobble position can restrict or expand the number of bases with which they can pair[4]. One such nucleotide located in position 34 is the hypermodfied nucleoside 2-Amino-5-[[[(1S,4S,5R)-4,5-dihydroxy-1-cyclopent- 2-enyl]amino]methyl]- 7-[(2R,3R,4S,5R)- 3,4-dihydroxy-5-(hydroxymethyl)- 2-tetrahydrofuranyl]-1H-pyrrolo[3,2-e]pyrimidin-4-one, queuosine. Queuosine is found in tRNAs with the GUN anticodon consensus sequence ($tRNA_{asp}$, $tRNA_{asn}$, $tRNA_{his}$, $tRNA_{tyr}$) and serves

as a structurally constraining base for tRNA codon loop flexibility. Queuosine is an essential micronutrient obtained by eukaryotes from diet or gut bacteria[5,6].

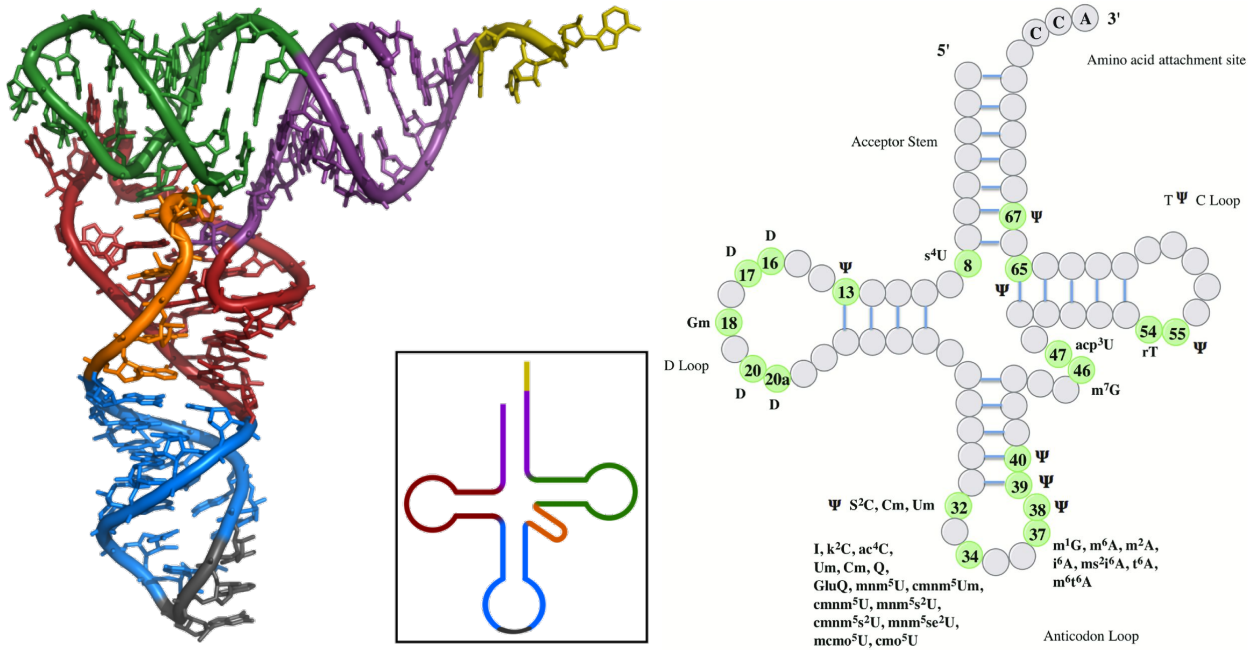

Figure 1: Two common models for describing tRNA structure. tRNA secondary structure displaying the locations of common nulcotide modifications(right). tRNA secondary structure and tertiary structure(left).

QueF

The first portion of the queusoine biosynthetic pathway begins with the medication of guanosine triphosphate (GTP) to 7-cyano-7-deazaguanine ($PreQ_0$). 7-cyano-7-deazaguanine reductase (QueF) (Figure 2) is the enzyme responsible for the reduction of the cyano group, (Figure 3; shown red), in $PreQ_0$ to form 7-aminomethyl-7-deazaguanine ($PreQ_1$) by two hydride transfers from the redox cofactor NADPH[7] (Figure 4). Notably, QueF is the only known example of biological nitrile reduction[8]. $PreQ_1$ is further modified by enzymes in the pathway and ultimately inserted into the tRNA (Figure 3). QueF is a

Figure 2: QueF pentamer quaternary structure. Monomers are identical, colored here to show assembly.

member of the Tunneling-fold (T-fold) super family. T-fold proteins bind substrates belonging to purine and pterin families. Their monomers consist of two alpha helicies layered onto the concave side of a four strand antiparallel beta sheet. Multiple monomers come together to form a barrel and two barrels combine head on to form the final multimeric tunnel[9]. The number of individual domains varies within the T-fold family, and size exclusion studies and X-ray crystal structures have shown QueF to be a homodecamer[10,8].

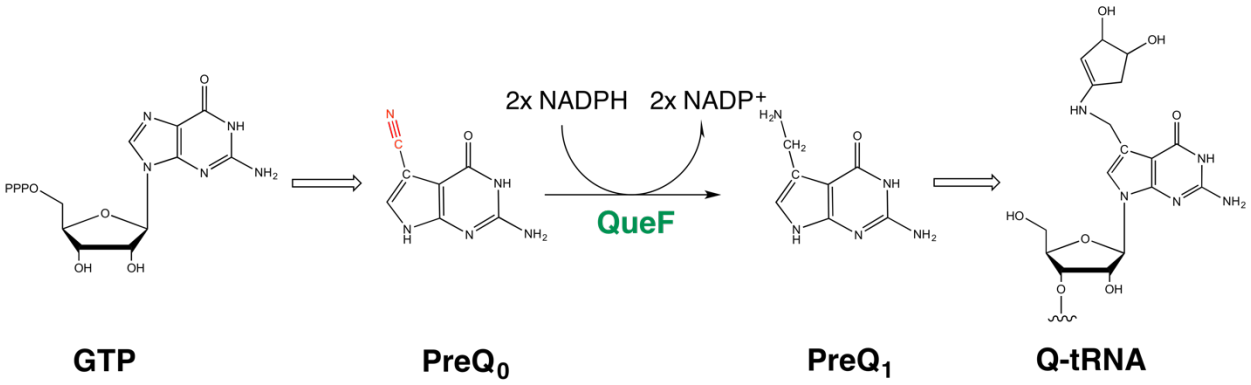

Figure 3: QueF's role in the queuosine bacterial biosynthetic pathway.

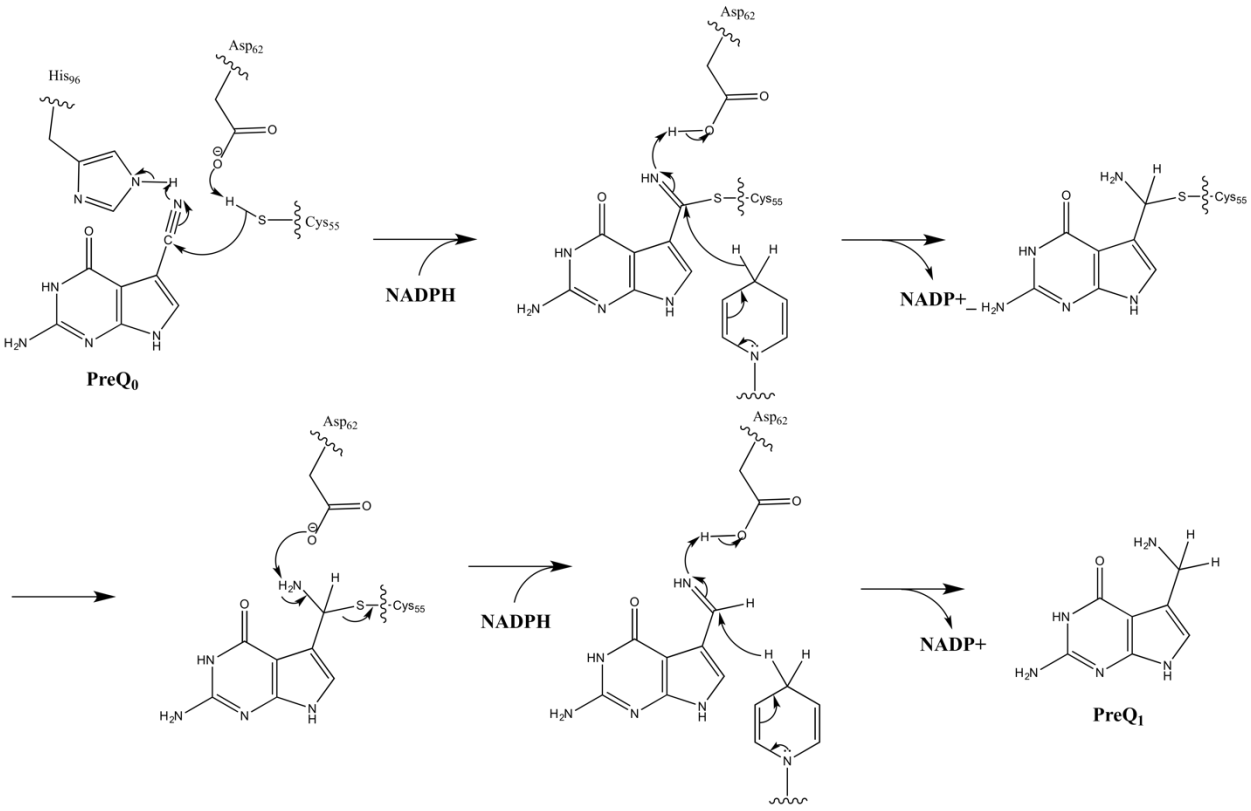

Figure 4 Reaction mechanism of the reduction of PreQ0 by QF. His_{96} and Asp_{62} act as proton donors/acceptors and Cys_{55} forms the thioimide intermediate with the nitrile group in the first step of the reaction.

Application

Conventional industrial nitrile reduction involves hydrogenation over a metal catalyst or by metal hydride reduction[11,12]. Enzymes have the ability to operate in an aqueous environment at physiological temperature and pressure. To satisfy increasing green chemistry standards, the demand for biocatalysts in product synthesis, extraction, purification and waste treatment is increasing[13]. Relaxing cofactor specificity is important to the use of QueF as a biocatalyst. NADPH and NADH are identical molecules aside from the presence of a phosphate group at the 2' position of the ribose ring that carries the adenine moiety in NADPH. NADPH costs over $10,000/mmol where as NADH costs near $380/mmol (Sigma 2015). This high cofactor price can be further reduced by developing NADH regenerative systems to be used in parallel with the catalyst[14].

Methods for engineering an enzyme for industrial use typically include directed evolution, rational design or a combination of the two[15]. Directed evolution mimics the process of evolution by introducing mutations and selecting variants with the desired function by application of a selective pressure. This method can be performed *in vivo* and *in vitro*. Rational design involves logically altering the structure of a protein through the site specific change in identity of target amino acid residues in order to alter the characteristics of the enzyme. Rational design was the method chosen for altering cofactor specificity in this project.

Experimental Design

Analysis of QueF cofactor docking models suggests an asymmetrical interaction between the decamer and NADPH (Figure 4). This interaction is comprised of the cofactor binding in the crease formed by three of the ten subunits, the nicotinamide group of NADPH positioned near the active site. Residues Q60 and Y21 appear to play an integral role in NADPH specificity. Q60 and Y21 of one subunit appear to interact with the 2'-phosphate of NADPH while the same residues of an adjacent subunit appear to interact with the 2'-hydroxyl of the nicotinamide ribose. This presents a unique challenge in rational design, as where it would be advantageous to alter the interaction at the site of the phosphate, a change here may also alter interaction at the ribose. Site directed mutagenesis and subsequent steady state kinetic analysis will be utilized to determine the residue's function in relation to cofactor binding and specificity. Q60 and Y21 will be mutated to alanine residues to establish their importance in cofactor binding. The residues will then be changed to amino acids with slightly different steric and electronic qualities (Q60A, Q60E, Q60N, Y21A, Y21F).

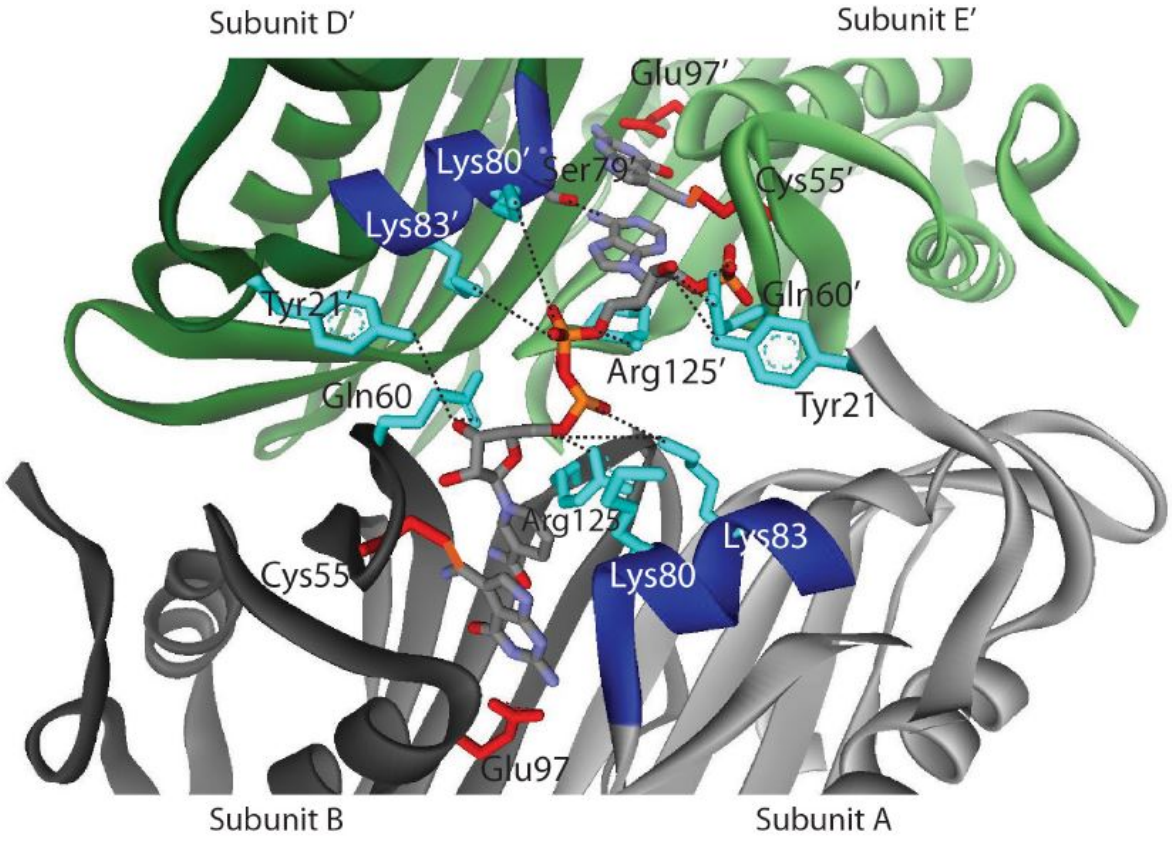

Figure 5 QueF substrate docking model.

Altering the sequence of amino acids within a protein can have a number of effects on its structure. The mutation can cause the protein to miss-fold, distorting the global structure of the monomer. This distortion can cause the protein to aggregate or prevent the mutant from otherwise forming the homodecamer, rendering it incapable of performing catalysis. Mutations may also distort the substrate binding pocket which can either affect substrate binding or the subsequent thioimide formation. Finally, the mutation can distort the cofactor binding pocket and alter cofactor binding or specificity.

To insure each mutant can still form a homodecamer their ability to bind substrate and form thioimide was assessed. The ability to form a thioimide bond with substrate can be used to confirm that the quaternary structure is intact as the active site is comprised of four monomers, two from each barrel. Inability to form thioimide indicates either the substrate binding pocket has been disrupted or the monomers cannot assemble to form the homodecamer. Steady state kinetics analysis was used to determine the effect of the mutation on the the enzymes ability to bind the cofactor as well as its ability to perform the necessary chemistry to carryout the reaction. In addition to NADPH turnover assays, all

mutants were subject to NADH turnover assays to determine if substrate specificity had been altered by the mutation.

Methods and Materials

General

Olgionucleotide synthesis was carried out by Integrated DNA Technologies, and sequencing was conducted by the Core Sequence Facility of Oregon Health and Science University. Protein concentrations were determined by UV-Vis spectroscopy on a Cary 100 Bio UV-Visible spectrophotometer, extinction coefficients were generated with Expasy ProtParam and confirmed by Bradford assay[16,17].

Growth conditions

Cell cultures were grown at 37°C in LB with kanamycin (50ug/ml).

Mutagenesis-Transformation

Site-directed mutagenesis was conducted using the Quick Change Mutagenesis Kit II (Agilent Technologies)[18]. Plasmids were transformed into NovaBlue (Novagen) competent cell for plasmid production, confirmed by Sanger sequencing and transformed into BL21 (Novagen) competent cells for protein over-production.

Enzyme	Sequence
Q60	5'-TTATGTCCTAAAACAGGCCAGCCTGACTTTGCGACAATCT-3'
Q60A	5'-TTATGTCCTAAAACAGGCGCGCCTGACTTTGCGACAATCT-3'
Q60N	5'-TTATGTCCTAAAACAGGCAACCCTGACTTTGCGACAATCT-3'
Q60E	5'-TTATGTCCTAAAACAGGCGAGCCTGACTTTGCGACAATCT-3'
Y21	5'- GGCAATCAAGGTACAAATTATTTGTTCGAATATGCACCGG-3'
Y21A	5'-GGCAATCAAGGTACAAATGCTTTGTTCGAATATGCACCGG-3'
Y21F	5'- GGCAATCAAGGTACAAATTTTTTGTTCGAATATGCACCGG-3'
C99	5'-GGTGACTTCCACGAGGACTGCATGAATATCATCATGAACG-3'
C99A	5'-GGTGACTTCCACGAGGACGCCATGAATATCATCATGAACG-3'
C99S	5'-GGTGACTTCCACGAGGACAGCATGAATATCATCATGAACG-3'

Table 1 List of mutant primers used

Protein production-purification

Cultures of wild type and mutant QF protein were grown for eight hours to an A_{600} of 3-4. Cells were pelleted (5Kg x 15min) and resuspended in an equivalent volume of media. Following 30-60 minutes of resuspension the cells were induced at a final concentration of 1 mM IPTG for four hours.

Post induction cells were harvested by centrifugation (10000g for 20 mins) and resuspended in purification buffer (100 mM Tris-HCl pH 8.0, 100 mM KCl, 2 mM ß-mercaptoethanol) supplemented with with 1mM PMSF and 250 μg/mL lysozyme to a final concentration of 250 g/mL. The resulting solutions were centrifuged (20Kg x 20min) and the supernatant applied to prequilibrated 5ml Ni-NTA (Qiagen) columns. Once loaded, the column was washed with 10CV purification buffer + 1 mM PMSF, 10CV purification buffer +20 mM imidazole, and the protein was eluted with 5CV purification buffer +200 mM imidizole. The protein was concentrated and the imidazole was removed from the elution fraction by dialysis (SnakeSkin dialysis tubing) against purification buffer, and stored at -80°C. Glycerol was added to 50% of the purified protein.

Turnover assays and relative activity

Consumption of NADPH was measured by loss of absorbance at 340 nm (ε=6220 $M^{-1}cm^{-1}$). Reaction was carried out at 37°C in 100 mM potassium phosphate (pH 6.5), 50 mM KCl, 20 mM $MgCl_2$ and 1 mM DTT. Wild type (WT) (200 nM) and mutant enzymes (20 μM) were incubated with 100 μM $PreQ_0$ for two minutes. Reaction was initiated with 180 μM NADPH and monitored for 10 minutes.

Thioimide formation

The thioimide bond forms a unique chromophore centered at 376 nm. Reaction mixtures were scanned between 230 and 420 nm to determine the extent of bond formation. Assay conditions were 100 mM phosphate (pH 6.5), 50mM KCl, 20 mM $MgCl_2$ and 1mM DTT. Enzyme at 20 μM was saturated with 100 μM $PreQ_0$.

NADH turnover assays

Consumption of NADH was measured by loss of absorbance at 340 nm (ε=6220 $M^{-1}cm^{-1}$). Reaction was carried out at 37°C in 100 mM potassium phosphate (ph 6.5), 50 mM KCL, 20 mM $MgCl_2$ and 1 mM DTT. Wild type (WT) (200 nM) and mutant enzyme (20 μM) were incubated with 100 μM $PreQ_0$ for two minutes. Reaction was initiated with 180 μM NADH and monitored for 10 minutes.

Steady-state kinetic analysis – NADPH

Reaction mixtures of 150 μL were comprised of 100mM phosphate (pH 6.5), 50mM KCl, 20mM $MgCl_2$, 1 mM DTT, 400 nM WT enzyme (800 nM mutant), 20 μM $PreQ_0$ and variable NADPH (10-200 μM). Reactions were initiated by adding 10 μL substrate mix (PreQ0 and NADPH) to 140 μL of enzyme mix (buffer, KCl, $MgCl_2$, DTT). Both solutions were pre incubated to 37°C for 5 min prior to mixing by pipette in a quartz cuvette. The reaction was monitored at 340 nM for 15 minutes and held at 37°C. Experiments were run in triplicate. Background oxidation rates of NADPH were monitored using final reaction mixtures minus enzyme. The rate of NADPH oxidation (Figure 6) were fit to a standard Michaelis-Menten curve (Eqn 1) (Figure 7) with KaleidaGraph software. Error for kcat and kcat/Km values was calculated using standard error propagation methods.

$$\nu = \frac{V_{max}[S]}{K_m + [S]} \quad \text{Equation 1}$$

Results

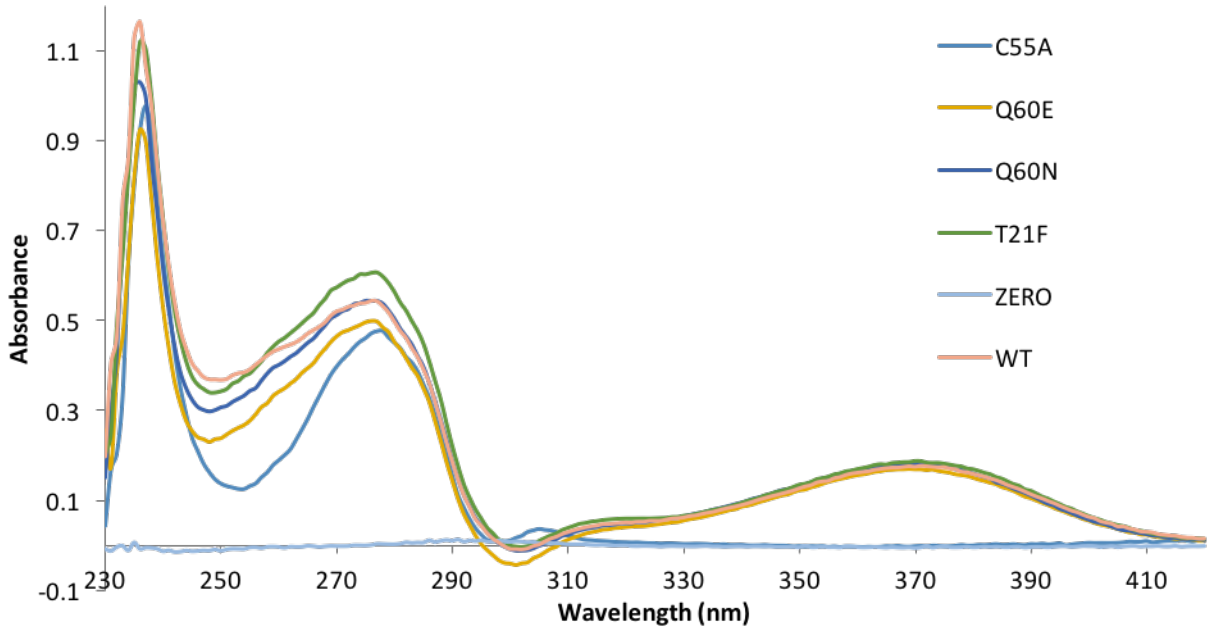

Figure 5 Thioimide formation of WT and mutant QueF

T21F, Q60N, Q60E and WT were able to form a thioimide bond (376 nm) with $PreQ_0$. C55A, lacking the nucleophilic cysteine residue was unable to form thioimide and was used as a control.

Enzyme	NADH oxidation ($\mu M*min^{-1}$)
Q60E	0.64
Q60N	0.55
Y21F	0.63
C55A	0.72
BACKGROUND	0.65
WT	0.77

Table 2 NADH oxidation by QueF WT and mutant

Under saturating conditions of $PreQ_0$, working with in the limits of the NADPH assay and an enzyme increase 12.5 fold, neither WT or mutant enzymes showed any reductive activity under the presence of NADH. The NADH oxidation rates for each enzyme are available in Table 2.

Enzyme	V_{max} ($\mu mol*min^{-1}$)	Km (μM)	k_{cat} (min^{-1})	K_{cat}/Km ($min^{-1}\ \mu M^{-1}$)
WT	1.52 ± 0.11	58.21 ± 10.87	1.89 ± 0.38	3.26E-02 ± 8.93E-03
Q60A	1.80 ± 0.36	329.63 ± 93.90	1.13 ± 0.39	3.42E-03 ± 1.54E-03
Q60N	0.79 ± 0.09	113.62 ± 25.58	0.50 ± 0.13	4.36E-03 ± 1.47E-03
Y21A	1.74 ± 0.20	178.23 ± 35.03	1.08 ± 0.25	6.09E-03 ± 1.83E-03
Y21F	1.66 ± 0.10	80.71 ± 10.60	1.03 ± 0.15	1.28E-02 ± 2.50E-03

Table 3 Kinetic parameters of WT and mutant QueF

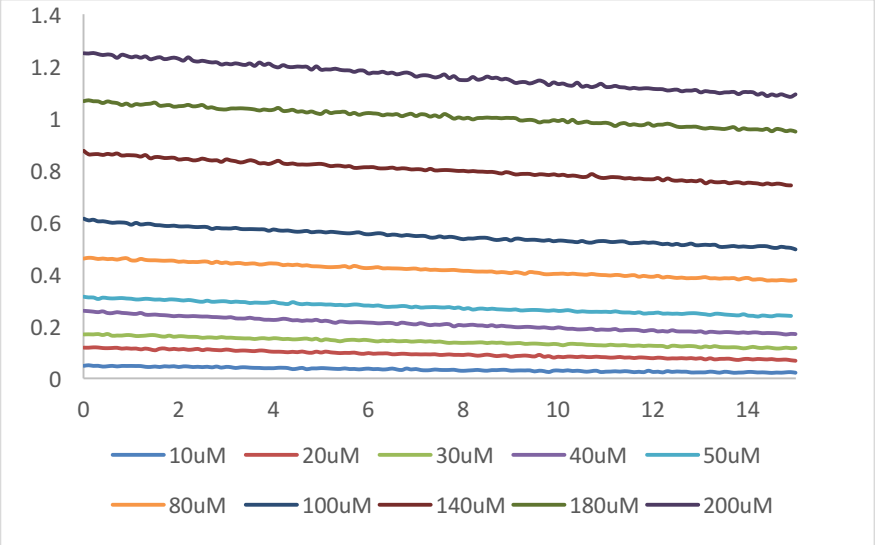

Figure 6 NADPH oxidation data used to determine reaction rates at different cofactor concentrations

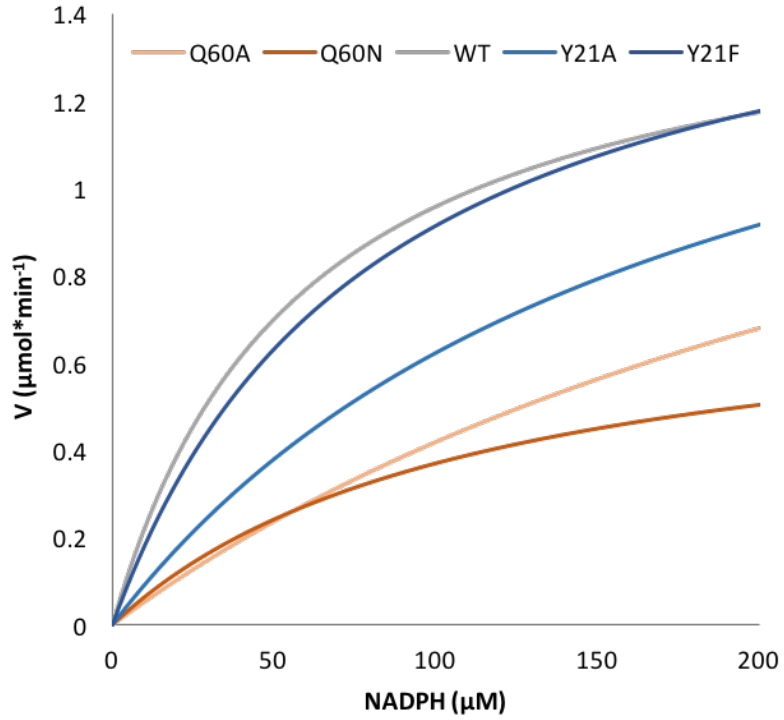

Figure 7 Michaleis-Menten curve comparison of QueF WT and mutant enzymes. Full Michaelis-Menten curves available in supplemental figures

$$k_{cat} = \frac{V_{max}}{[E]_0} \quad \text{Equation 2}$$

Despite not having discrete on and off rates we can use the Km to approximate the Kd. The k_{cat} was determined using Equation 2. Q60A Km is 5.7 times WT and has a k_{cat} 59% of WT, indicating a decrease in cofactor affinity and reduction in the rate of catalysis. Q60N Km is 1.95 times WT and has a k_{cat} 26% of WT, indicating an affinity for cofactor greater than Q60A but less than that of WT and a rate of catalysis lower than Q60A and WT. Q60E activity was too low to yield any kinetic data from this experiment. However, under enzyme concentrations 62.5 times higher (25 µM) a rate 4 times slower that WT was observed yielding a 250-fold decrease in activity. Y21A Km is 3.06 times WT and has k_{cat} 57% of WT indicating a decrease in cofactor affinity and reduciton in the rate of catalysis. Y21F Km is 1.39 times WT and has k_{cat} 54% of WT, indicating a lesser reduction of affinity for cofactor than in Y21A and a similar decreased rate of catalysis.

Discussion

NADH turnover assay

No mutants were able to utilize NADH as a cofactor for PreQ0 reduction. This is in contrast to the hypothesis that residues Q60 and Y21 played a specific, distinct role in cofactor specificity. The inability of neither WT or mutant QueF may implicate that these residues interact with the phosphate moiety to stabilize and position NADPH to allow for proper hydride transfer.

Steady state kinetic analysis

The k_{cat} can be used to represent the catalytic velocity of the enzyme under ideal, saturated conditions. Individual on and off rates (Figure 7) cannot be determined using steady-state kinetic analysis. Despite not having discrete on and off rates we can use the Km to approximate the Kd. The Kd being the ratio of the on and off rates of the ES complex, in this case the ES+NADPH complex. The lower the Kd, here the Km, the higher the enzyme's affinity for the substrate. The ratio of k_{cat}/Km is a measure of catalytic efficiency, a fast enzyme and or one that can bind substrate at low concentrations will be a more efficient enzyme and will there have a larger ratio of k_{cat}/Km. Although the docking model shows targeted residues do not directly interact with PreQ0 binding, without steady-state kinetic analysis of $PreQ_0$ binding we cannot claim that the mutated residues do not have any concurrent effect on $PreQ_0$ interaction.

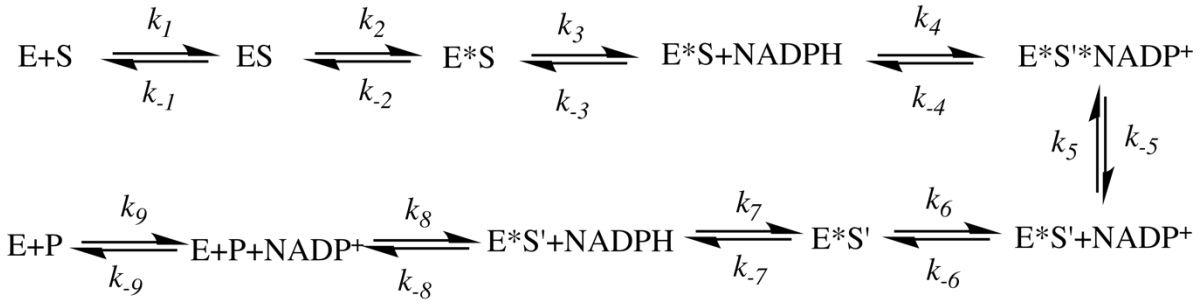

Figure 8 QueF kinetic scheme

At the time of discovery, initial characterization determined the WT Km for NADPH to be 36µM and the k_{cat} to be 0.6 min^{-1} (100mM Hepes pH 7.5, 1 mM DTT, 50-100 mM KCl at 30°C).[19] A second characterization of WT after metal binding studies showed the Km and V_{max} to be 19.2±1.07 µM and 0.69±0.02 min^{-1}, respectively (100 mM TRIS pH 7.5, 100 mM KCl, 1mM DTT 20 µM $PreQ_0$, 0.776 µM WT QueF for 120s at 30°C)[7]. Both assessments used the continuous UV-vis assay employed in this experiment. The disparity between the rates achieved in this experiment, Km: 58.21±10.87 µM and k_{cat}: 1.89±0.38 min^{-1}, compared

to those of past papers can be attributed to the different conditions, mainly the pH of the reaction buffer. Studies following the first two characterizations and preceding this experiment determined optimal enzyme activity proceeded at pH 6.5.

Q60A, having essentially all steric and electric influence eliminated had a much larger Km, nearly 6X of WT and it's k_{cat} was 59% of WT. This is supports the relationship posed by the docking model that Q60 has a role in coordinating cofactor binding/positioning. The decrease in k_{cat} may be a product of diminished ability to position the substrate by interaction with the 2'OH of the ribose on the subunit proximal to the active site.

The Q60N mutant would draw the amide side-chain towards the protein backbone. Consistent with the hypothesis, the Km was greater than WT but less than Q60A, indicating an affinity for cofactor somewhere in between WT and the alanine mutant. Interestingly, the k_{cat}, at 26% of WT, was lower than that of the alanine mutant. This may indicate that Q60 may play an important role in positioning the NAPDH appropriately for hydride transfer. If the R-group of glutamine acts as a positive cup to cradle the negatively charged phosphate, then the shorter R-group of asparagine may position the nicotinamide moiety unfavorable, thereby preserving the affinity for substrate yet reducing the overall catalytic rate.

The Q60E mutant may be the most important in supporting the hypothesis that Q60 interacts with the cofactor phosphate. With 250X less activity than wild type its kinetic parameters were unable to be experimentally derived. Such a reduction in activity may be attributed to the change in the side chain function group from an amide to a carboxylate. This strong negative charge of the side chain and the negative charge of the phosphate group would likely repulse each other, making docking of the cofactor unfavorable and thereby nearly eliminating its ability to bind cofactor and perform catalysis. Thioimide forming studies eliminate the possibility that the Q60E mutation impacted the global structure of the enzyme since $PreQ_0$ binding is essentially unperturbed.

The kinetic data for Y21A and Y21F supported the hypothesis that they have some affect on cofactor docking and binding. The greater the deviation from the tyrosine side-chain structure the higher the Km, possibly revealing the steric importance of Y21 in binding/docking NADPH. The k_{cat} of the alanine and phenylalanine mutants were similar at 54% and 57% of WT, respectively. This decrease in k_{cat} may be due to decreased unfavorable positioning of the substrate.

This data provides in vitro support that Q60 and Y21 effect cofactor binding, if not in cofactor scpecifcity than in positioning of cofactor for catalysis of $PreQ_0$ to $PreQ_1$. Future studies should include $PreQ_0$ kinetic

analysis of Gln60 and Tyr21 mutants to determine if these residues impact substrate binding rates. Transient kinetic studies of NADPH and NADH binding in WT and mutants may further elucidate the role of these residues.

Additional Figures

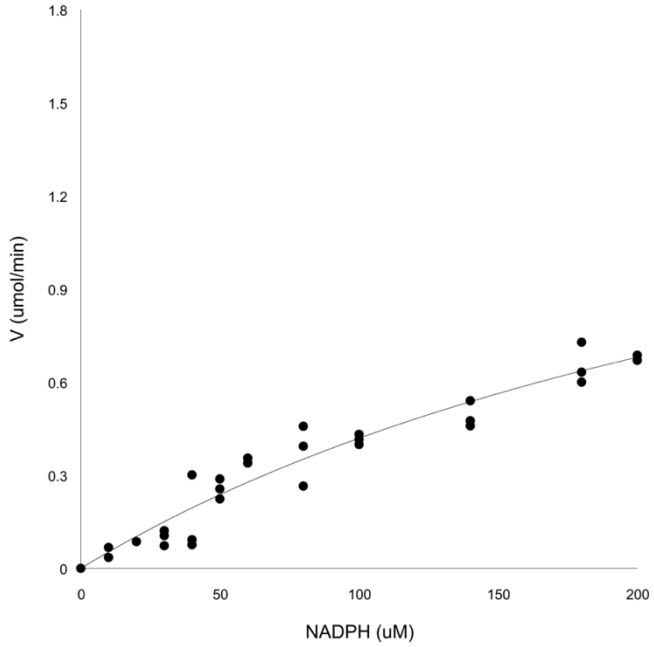

Figure 9 Q60A saturation curve

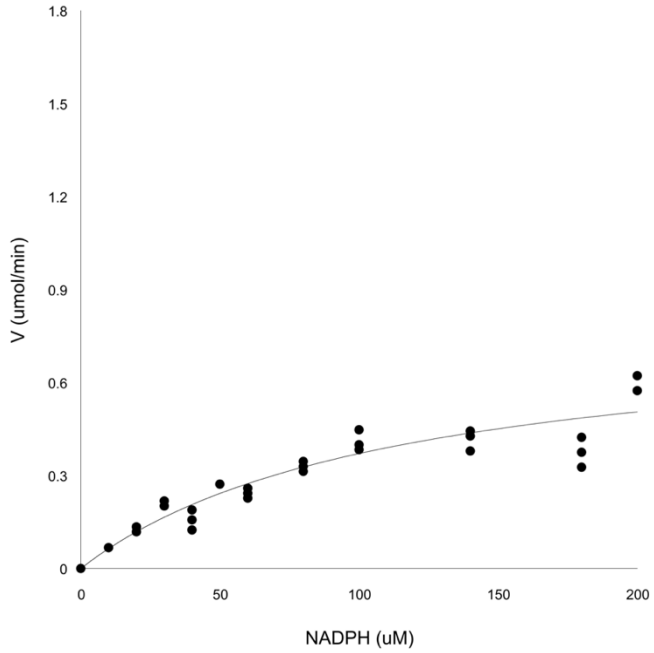

Figure 10 Q60N saturation curve

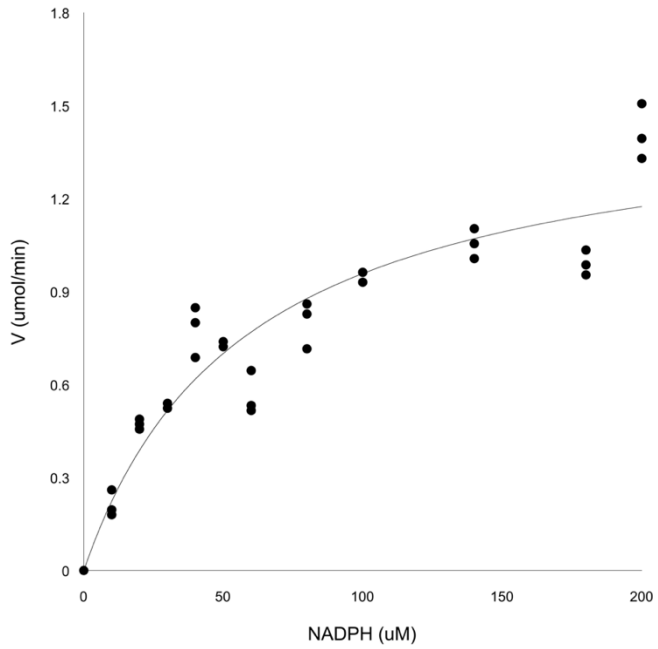

Figure 11 WT saturation curve

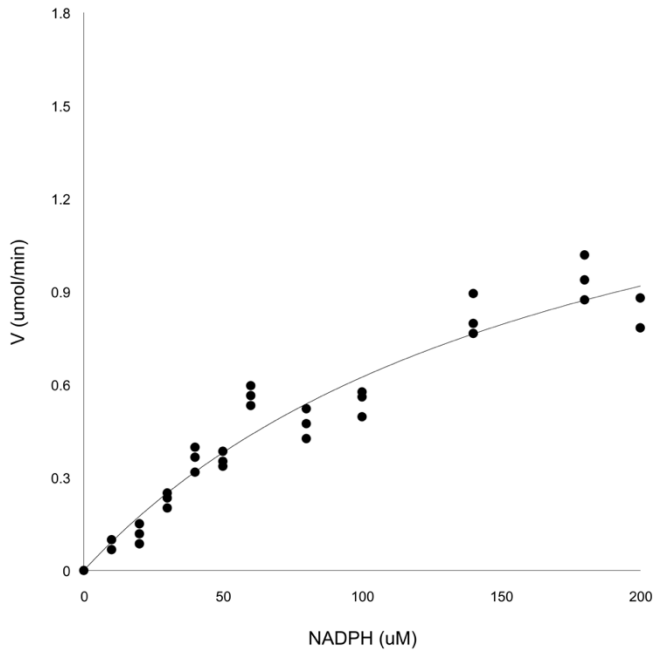

Figure 12 Y21A saturation curve

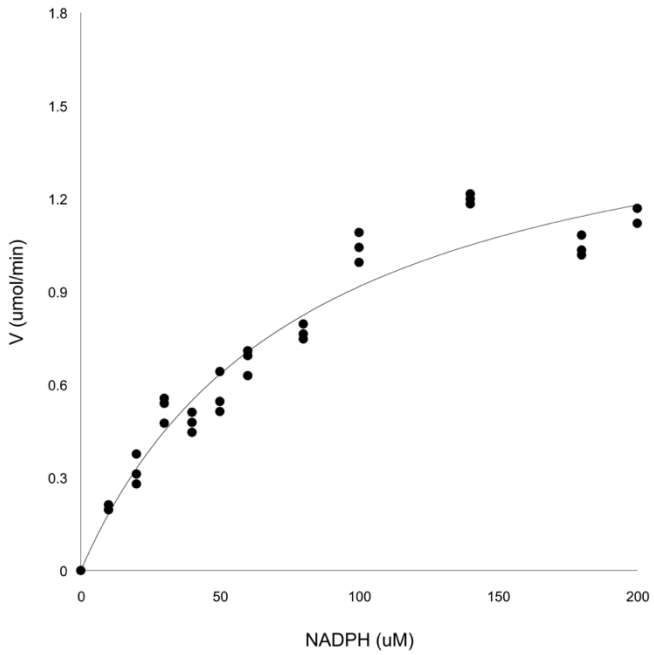

Figure 13 Y21F saturation curve

Work Cited

1. Agris, P. F. Decoding the genome: A modified view. *Nucleic Acids Res.* **32,** 223–238 (2004).
2. Woese, C. R., Olsen, G. J., Ibba, M. & Söll, D. Aminoacyl-tRNA Synthetases, the Genetic Code, and the Evolutionary Process. *Microbiol. Mol. Biol. Rev.* **64,** 202–236 (2000).
3. Osawa, S., Jukes, T. H., Watanabe, K. & Muto, A. Recent evidence for evolution of the genetic code. *Microbiol. Rev.* **56,** 229–64 (1992).
4. Agris, P. F., Vendeix, F. a P. & Graham, W. D. tRNA's Wobble Decoding of the Genome: 40 Years of Modification. *J. Mol. Biol.* **366,** 1–13 (2007).
5. Zallot, R. *et al.* Plant, Animal, and Fungal Micronutrient Queuosine Is Salvaged by Members of the DUF2419 Protein Family. *ACS Chem. Biol.* (2014). doi:10.1021/cb500278k
6. Morris, R. C., Brown, K. G. & Elliott, M. S. The effect of queuosine on tRNA structure and function. *J. Biomol. Struct. Dyn.* **16,** 757–774 (1999).
7. Lee, B. W. K., Van Lanen, S. G. & Iwata-Reuyl, D. Mechanistic studies of Bacillus subtilis QueF, the nitrile oxidoreductase involved in queuosine biosynthesis. *Biochemistry* **46,** 12844–12854 (2007).
8. Chikwana, V. M. *et al.* Structural basis of biological nitrile reduction. *J. Biol. Chem.* **287,** 30560–30570 (2012).
9. Colloc'h, N., Poupon, A. & Mornon, J. P. Sequence and structural features of the T-fold, an original tunnelling building unit. *Proteins Struct. Funct. Genet.* **39,** 142–154 (2000).
10. Chikwana, V. M. Discovery of Novel Amidotransferase Activity Involved In Archaeosine Biosynthesis and Structural and Kinetic Investigation of QueF , an Enzyme Involved in Queuosine Biosynthesis. (2011).
11. Haddenham, D., Pasumansky, L., Desoto, J., Eagon, S. & Singaram, B. Reductions of Aliphatic and Aromatic Nitriles to Primary Amines with Diisopropylaminoborane Reductions of Aliphatic and Aromatic Nitriles to Primary Amines with Diisopropylaminoborane. **74,** 1964–1970 (2009).
12. Werkmeister, S., Bornschein, C., Junge, K. & Beller, M. Ruthenium-catalyzed transfer hydrogenation of nitriles: Reduction and subsequent N-monoalkylation to secondary amines. *European J. Org. Chem.* 3671–3674 (2013). doi:10.1002/ejoc.201300151
13. Schmid, a *et al.* Industrial biocatalysis today and tomorrow. *Nature* **409,** 258–268 (2001).
14. Woodyer, R., Van der Donk, W. a. & Zhao, H. Relaxing the nicotinamide cofactor specificity of phosphite dehydrogenase by rational design. *Biochemistry* **42,** 11604–11614 (2003).
15. Zhao, H., Chockalingam, K. & Chen, Z. Directed evolution of enzymes and pathways for industrial biocatalysis. *Curr. Opin. Biotechnol.* **13,** 104–110 (2002).
16. Gasteiger, E. *et al.* Protein Identification and Analysis Tools on the ExPASy Server. *Proteomics Protoc. Handb.* 571–607 (2005). doi:10.1385/1-59259-890-0:571
17. Bradford, M. M. A rapid and sensitive method for the quantitation of microgram quantities of protein utilizing the principle of protein-dye binding. *Anal. Biochem.* **72,** 248–254 (1976).
18. Dhuffman. Manual: QuikChange II Site-Directed Mutagenesis Kit. **200523,** 1–19 (2010).
19. Van Lanen, S. G. *et al.* From cyclohydrolase to oxidoreductase: discovery of nitrile reductase activity in a common fold. *Proc. Natl. Acad. Sci. U. S. A.* **102,** 4264–4269 (2005).